

# Proangiogenic Hydrogels Within Macroporous Scaffolds Enhance Islet Engraftment in an Extrahepatic Site

Ann-Christina Brady, MD,<sup>1,2</sup> Mikael M. Martino, PhD,<sup>3</sup> Eileen Pedraza, PhD,<sup>1,4</sup>  
Steve Sukert, BS,<sup>1</sup> Antonello Pileggi, MD, PhD,<sup>1,2,4,5</sup> Camillo Ricordi, MD,<sup>1,2,4-6</sup>  
Jeffrey A. Hubbell, PhD,<sup>1,3,7</sup> and Cherie L. Stabler, PhD<sup>1,2,4</sup>

The transplantation of allogeneic islets in recent clinical trials has shown substantial promise as a therapy for type 1 diabetes; however, long-term insulin independence remains inadequate. This has been largely attributed to the current intravascular, hepatic transplant site, which exposes islets to mechanical and inflammatory stresses. A highly macroporous scaffold, housed within an alternative transplant site, can support an ideal environment for islet transplantation by providing three-dimensional distribution of islets, while permitting the infiltration of host vasculature. In the present study, we sought to evaluate the synergistic effect of a proangiogenic hydrogel loaded within the void space of a macroporous poly(dimethylsiloxane) (PDMS) scaffold on islet engraftment. The fibrin-based proangiogenic hydrogel tested presents platelet derived growth factor (PDGF-BB), via a fibronectin (FN) fragment containing growth factor and major integrin binding sites in close proximity. The combination of the proangiogenic hydrogel with PDMS scaffolds resulted in a significant decrease in the time to normoglycemia for syngeneic mouse islet transplants. This benefit was associated with an observed increase in competent vessel branching, as well as mature intraislet vessels. Overall, the addition of the proangiogenic factor PDGF-BB, delivered via the FN fragment-functionalized hydrogel, positively influenced the efficiency of engraftment. These characteristics, along with its ease of retrieval, make this combination of a biostable macroporous scaffold and a degradable proangiogenic hydrogel a supportive structure for insulin-producing cells implanted in extrahepatic sites.

## Introduction

CONVENTIONAL MEDICAL TREATMENT for type 1 diabetes, based on exogenous insulin and frequent glucose monitoring, is unable to adequately control glycemia to prevent secondary complications.<sup>1</sup> Current clinical islet transplantation (CIT) trials exhibit superior control in blood glucose levels and insulin independence in patients with brittle type 1 diabetes.<sup>2,3</sup> The promising results of recent trials are dampened, however, by the high islet demand per patient, significant early islet loss, and moderate long-term function.<sup>4</sup> Embolization into the hepatic portal system has been proven to be a nonideal site, as islets are exposed to undesirable conditions, such as high drug and toxin loads, mechanical stress, and an acute inflammatory blood-mediated response.<sup>5-7</sup>

As such, there are efforts to develop an alternative site for islet cell transplantation that would minimize exposure of islets to these detrimental conditions. Several sites and im-

plant designs have been explored. Popular sites include the kidney capsule, omental pouch, epididymal fat pad, intramuscular, and peritoneum (see reviews<sup>8,9</sup>). Device configurations for housing islets have ranged from beads, to rods, to sheets, to disks, with various materials employed from degradable extracellular matrices to alginate hydrogels (see reviews<sup>10-12</sup>).

In the fabrication of macroscale devices for housing islets, early studies focused on immunoisolating devices, a particular challenge given that islet revascularization and engraftment are prevented. Recent approaches, however, have sought to generate an integrated islet graft site through the use of macroporous scaffolds.<sup>13-15</sup> This approach seeks to create intimacy between the islets and the surrounding environment, while also providing a platform for modulation and control of the local transplant site. Our laboratory has demonstrated, in rat and nonhuman primate models, that the use of a poly(dimethylsiloxane) (PDMS) macroporous

<sup>1</sup>Diabetes Research Institute, University of Miami, Miami, Florida.

<sup>2</sup>Department of Surgery, University of Miami, Miami, Florida.

<sup>3</sup>Institute of Bioengineering, School of Life Sciences and School of Engineering, Ecole Polytechnique Fédérale de Lausanne (EPFL), Lausanne, Switzerland.

Departments of <sup>4</sup>Biomedical Engineering, <sup>5</sup>Microbiology and Immunology and <sup>6</sup>Medicine, University of Miami, Miami, Florida.

<sup>7</sup>Institute of Chemical Sciences and Engineering, School of Basic Sciences, Ecole Polytechnique Fédérale de Lausanne (EPFL), Lausanne, Switzerland.

scaffold within an alternative transplant site can be highly effective in restoring normoglycemia.<sup>15–17</sup> The use of PDMS, a material with a long-standing clinical profile, has the advantages of biostability, thereby preserving retrievability, as well as ease in delivering beneficial agents, such as anti-inflammatory and immunomodulatory agents, and/or oxygen, to the localized islet transplant environment.<sup>18,19</sup>

Of particular importance in designing implants for housing islets is promoting the development of competent vascular networks. This is desirable not only due to the high oxygen demand of islets,<sup>20,21</sup> but also to impart glucose responsiveness. Even when transplanted directly within the liver microvasculature, the delay in islet revascularization (from 7–14 days) for current CIT transplants results in hypoxia-induced islet apoptosis.<sup>22–25</sup> Exposure of islets to hypoxia results in activation of HIF-1 $\alpha$  pathways, which not only leads to cellular death, but also to stimulation of inflammatory pathways and impairment of glucose responsiveness.<sup>26–28</sup> Therefore, prompt revascularization of islet grafts is critical for transplant success.<sup>23</sup> As such, accelerating vascularization of these initially avascular islet-containing implants is of critical importance.

Several approaches have been investigated to enhance the local angiogenic potential within the graft.<sup>29–34</sup> The use of proangiogenic, degradable hydrogels through the combination of angiogenic growth factors (GFs), such as the platelet-derived GF (PDGF-BB) and vascular endothelial GF (VEGF), and biomaterials is an attractive approach that has shown enhanced therapeutic effect over delivery of GF alone.<sup>35–38</sup> Given the importance of islet revascularization in graft efficacy, we sought to explore the potential use of proangiogenic hydrogels within PDMS scaffolds at an alternative transplant site. We evaluated the ability of fibrin-based PDGF-BB-containing hydrogels to enhance engraftment efficiency, as well as competency of both intradvice and inraislelet vascularization, in a syngeneic mouse transplant model. The generality of this combinatory platform to enhance vascularization to tissue-engineered implants is also discussed.

## Materials and Methods

### Animals

All animal studies were reviewed and approved by the University of Miami Institutional Animal Care and Use Committee. All procedures were conducted according to the guidelines of the Committee on Care and Use of Laboratory Animals, Institute of Laboratory Animal Resources (National Research Council). Animals were housed within microisolated cages in virus antibody-free rooms with free access to autoclaved food and water at the Department of Veterinary Resources of the University of Miami. The Preclinical Cell Processing and Translational Models Core at the Diabetes Research Institute performed the rodent islet isolations, diabetes induction, and animal monitoring. Male C57BL/6J (B6) mice, between 10–12 weeks of age (Jackson Laboratory), were used as islet donors. Male C57BL/6J mice, between 7–9 weeks of age (Jackson Laboratory), were used as transplant recipients. Mice were rendered diabetic by intravenous administration of 200 mg/kg streptozotocin (STZ; Sigma) freshly dissolved in the citrate buffer and were used as recipients of syngeneic islets only if overtly diabetic upon three consecutive readings of nonfasting blood glucose levels

>350 mg/dL, using portable glucose meters (OneTouchUltra2; Lifescan).<sup>39</sup>

### Scaffold fabrication

Macroporous PDMS scaffolds were fabricated using the solvent casting and particulate leaching technique, as described elsewhere.<sup>15</sup> Briefly, PDMS polymer (RTV 615 A&B; GE Silicone) was prepared by mixing PDMS monomer with catalyst (4:1 v/v) and with salt, sieved to 250 to 425  $\mu$ m diameter, at a 90% v/v salt/PDMS ratio. The PDMS/salt paste was then loaded into prefabricated, silicone molds (10  $\times$  10 mm; 2 mm height), compressed, and incubated at 37°C for 48 h. Salt was leached from scaffolds via soaking in deionized water for 5 days, with water changes every 24 h. Scaffolds were then dried, cut into 5  $\times$  5-mm squares, and steam sterilized. Before implant, the hydrophobic PDMS was coated with human fibronectin (FN; Gibco) via incubation in a 250  $\mu$ g/mL solution.

### Fibrin hydrogel with PDGF-BB

The fibrin/PDGF-BB gel used in these studies to promote vascularization contained basic fibrin gel components, as well as a FN fragment and PDGF-BB. The FN fragment, containing both the FN III 9–10 and 12–14 sequence, labeled FN III9-10/12–14, was produced using methods described in previous publications.<sup>40, 41</sup> Details on its specific sequence are also published.<sup>41</sup> Fibrin/FN/PDGF-BB hydrogels were generated using methods previously described.<sup>40,41</sup> Briefly, a solution of PBS containing the FN fragment (155  $\mu$ g/mL) and PDGF-BB (2  $\mu$ g/mL; Invitrogen) was incubated for 30 min at RT to facilitate binding between the GF and the FN fragment. Concurrently, a solution containing thrombin (2 U/mL), factor XIII (8 U/mL), aprotinin (85  $\mu$ g/mL), 5 mM CaCl<sub>2</sub>, 150 mM NaCl, and 20 mM HEPES was incubated at 37°C for 15 min to activate factor XIII. This solution was then added to the FN/PDGF-BB mixture to form the crosslinking solution (28.5  $\mu$ L per 100  $\mu$ L of FN/PDGF-BB mixture). A second solution of fibrinogen (4 mg/mL) within a HEPES buffer (150 mM NaCl, 20 mM HEPES, pH 7.5) was made. At the time of loading onto the scaffold, the fibrinogen solution was added to the crosslinking solution at a 1:1 ratio. This solution was then loaded onto the scaffold, whereby it polymerized in <15 s.

For sealing the fat pads, a basic fibrin solution, free of GF and FN fragments, was made, whereby only fibrinogen (8 mg/mL), thrombin (2 U/mL), aprotinin (85  $\mu$ g/mL), and CaCl<sub>2</sub> (5 mM) were used.

### Cell isolation and culture

Islets were obtained from donor mice via mechanically enhanced enzymatic digestion, followed by density gradient purification, as previously described.<sup>39</sup> Islet purity was assessed by dithizone (Sigma) staining, and the islets were counted and scored for size using an algorithm for the calculation of the 150- $\mu$ m diameter islet equivalent (IEQ) number. Islets were cultured in the CMRL 1066-based medium (Mediatech) supplemented with 10% fetal bovine serum (FBS; Sigma), 1% penicillin–streptomycin (Sigma), and 1% L-glutamine (Sigma) for 24 h before seeding into scaffolds immediately before transplantation.

### Islet loading on scaffolds

Scaffolds were prepared for islet loading via washing with CMRL culture media. Islet aliquots, based on IEQ, were loaded into the fabricated scaffolds by concentrating islets into 15  $\mu$ L of media and seeding them onto the scaffolds, where they filtered through the micro-sized pores via gravity. Either 500 (full islet mass) or 250 IEQ (suboptimal islet mass) per scaffold was used, depending on the experiment. For the subset of scaffolds receiving the fibrin gel and PDGF-BB, 15  $\mu$ L of the liquid fibrin/PDGF-BB mix was added to the islet-loaded scaffolds by loading onto the top of the PDMS scaffold. The liquid filled the void spaces and gelled within. Following a 5-min incubation, scaffolds were then transferred to a well within a 24-well plate filled with 1.5 mL of media, and incubated in a humidified 37°C, 5% CO<sub>2</sub>/95% air incubator. Islet-loaded scaffolds were transplanted within 2–4 h following loading.

### Islet transplantation and graft assessment

Under general anesthesia (isoflurane USP; Baxter), a lower midline incision was made and the epididymal fat pad was mobilized, exposed, and spread using sterile saline. Three implant conditions were performed: free islets; islets loaded within PDMS scaffolds; and islets loaded within PDMS scaffolds plus fibrin/PDGF-BB. For free islets, the desired IEQ loading was concentrated within 15  $\mu$ L and dropped onto a section of the spread fat pad. The fat pad was then wrapped around the islets by folding each side inward and the edges were sealed using plain fibrin hydrogel (no GF). For islets loaded within PDMS scaffolds, a single islet-loaded scaffold was placed onto the exposed fat pad. The fat pad was then wrapped around the scaffold by folding each side inward (Fig. 1). The edges of the omental pouch were subsequently sealed with plain fibrin hydrogels. After 1 min, the fat pad was then placed back into the peritoneal cavity and the incision was sutured and stapled.

Normoglycemia of the recipients was defined as stable nonfasting glycemic levels <200 mg/dL for two consecutive readings.<sup>39</sup> Mice that remained hyperglycemic for over 100 days were considered nonfunctional and euthanized. For metabolic assessment, an intraperitoneal glucose tolerance test (IPGTT) was performed on day 95 in animals bearing a functional islet graft. After overnight fasting, mice received an intraperitoneal glucose bolus (2 g/kg in saline) and blood glucose was monitored until it read below 200 mg/dL (at least 90 min). Glucose clearance was evaluated by calculating

the area under the curve (AUC) from the first reading until 90 min. To ensure that the function observed in normoglycemic animals was due to the islet transplant, the graft-bearing fat pad was explanted in a survival surgery and the glycemic levels monitored to ensure the prompt return to a diabetic state.

For analysis of vascularization, 250 IEQ were loaded within either PDMS scaffolds or PDMS scaffolds plus fibrin/PDGF-BB. Grafts were explanted 10 and 30 days post-transplantation for immunohistochemical analysis of islet vascularization.

Histological analysis of explanted grafts was conducted following fixation in 10% formalin buffer, whereby grafts were then paraffin embedded and sectioned into 5- $\mu$ m-thick sections. Tissue sections were stained with hematoxylin and eosin, as well as Masson tri-chrome staining (Richard Allan Scientific). Immunofluorescence was used to image islets and vascularization. Staining for insulin was performed using polyclonal primary guinea pig anti-insulin (1:100; DAKO, A0564) and a secondary goat anti-guinea pig AlexaFluor-568- or AlexaFluor-647-conjugated antibody (Invitrogen A-21450 or A-11075). Blood vessels were detected via the rabbit CD31 monoclonal antibody (1:50; Abcam, ab28364) or the rabbit anti- $\alpha$ -smooth muscle actin (SMA) polyclonal antibody (1:50; Abcam, ab5694). Primary antibodies were detected using goat anti-rabbit AlexaFluor-488 (CD31)- or AlexaFluor-568 (SMA)-conjugated antibody (1:200; Invitrogen A-11008 or A-11036, respectively). Nuclei were stained using DAPI. All results were compared to isotype controls (primary antibody omitted) to ensure specificity of detection. Histological images were collected using a Zeiss LSM 510 confocal microscope or Leica SP5 spectral confocal inverted microscope. Due to the extreme difficulty in sectioning the PDMS scaffold and subsequent folding and smearing of the sectioned tissue, particularly at early time points due to lack of substantial host remodeling/infiltration, quantification of overall vascular staining was not feasible.

### Vessel perfusion

To evaluate functional and competent vascularization of scaffolds, PDMS scaffolds with or without fibrin/PDGF-BB were transplanted into the left and right epididymal fat pads, respectively, of the same animal. Ten days post-transplantation, vessel perfusion was performed using DiI (D-282; Invitrogen) following published methods.<sup>42</sup> Briefly, mice were euthanized via CO<sub>2</sub> inhalation before median

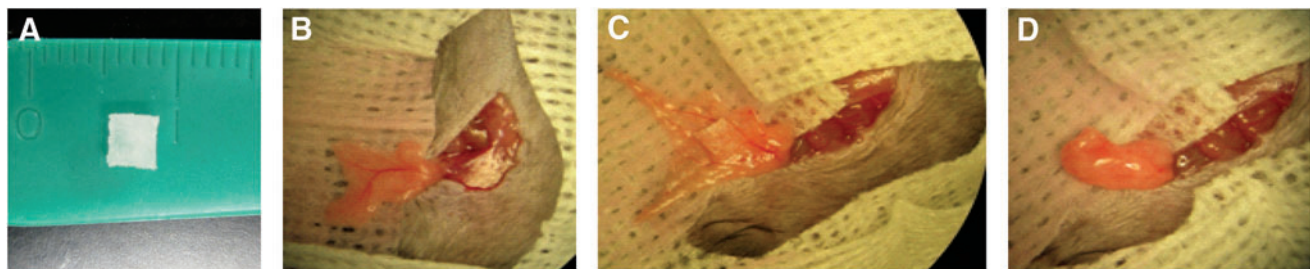


**FIG. 1.** Photographs of (A) poly(dimethylsiloxane) (PDMS) scaffold used for implantation (5×5×2 mm); (B–D) PDMS scaffold implantation into the epididymal fat pad site, where the PDMS scaffold containing islets, with or without fibrin/platelet-derived growth factor (PDGF-BB), was placed on spread fat pad, wrapped in the fat pad tissue, sealed with a plain fibrin gel (no growth factor), and placed back into the peritoneum. Color images available online at [www.liebertpub.com/tea](http://www.liebertpub.com/tea)



sternotomy and exposure of chest cavity. A butterfly needle, connected via a three-way stopcock to syringes containing PBS or DiI solution, was inserted into the left ventricle of the heart and the right atrium was subsequently punctured via a 16G needle, releasing venous blood return. Following flushing of the circulatory system with PBS (1.5 mL/min, ~2 mL), DiI was injected (1.5 mL/min, ~5 mL). Fat pads were explanted and fixed in 4% paraformaldehyde. Following fixation, grafts were flushed in saline and excess fat was trimmed from the implant. Using a stereomicroscope, the scaffold was then sectioned in half and a thin slice of this cross section was portioned. This scaffold cross section was then placed down onto a glass coverslip for imaging of vascular infiltration within the scaffold. Images were collected using a Leica SP5 spectral confocal inverted microscope. Multislice images (4–8- $\mu$ m thickness; 50–110 slices per image; 1024 $\times$ 1024; 10 $\times$  objective) were collected and compiled using three-dimensional projection function.

#### Statistical analysis

For time to reversal analysis (% normoglycemia), the Mantel-Cox (logrank) test was performed to evaluate differences between groups. Blood glucose results are expressed as the mean  $\pm$  SD, with the number of animals within each group indicated in the figure legend. For blood glucose time course analysis, repeated measure analysis of variance with Greenhouse–Geisser *post hoc* analysis for within subject effects was used (due to rejection of Mauchly's Test of Sphericity). The Levine's test of equality of error variance was used to compare homogeneity of variances. Differences were considered significant when  $p < 0.05$ .

## Results and Discussion

### Biodegradable, PDGF-BB releasing, fibrin-based hydrogel

In the development of proangiogenic hydrogels, we have investigated the use of FN fragments that express native binding sites for GFs, and integrins. Specifically, we have developed a system comprised of the fibrin network, angiogenic growth factors (PDGF-BB and VEGF-A), and a recombinant fragment of FN.<sup>40</sup> The FN fragment is engineered to contain (i) a factor XIIIa substrate fibrin-binding sequence; (ii) the 9th–10th type III FN repeat (FN III9–10) containing the major integrin-binding domain; and (iii) the 12th–14th type III FN repeat (FN III12–14), which binds GFs promiscuously, including VEGF A (referring to VEGF-A165) and PDGF-BB.<sup>40,41</sup> We have previously shown this novel system to provide potent synergistic signaling and morphogenesis between  $\alpha 5\beta 1$  integrin and GF receptors, when the FN III9–10 and FN III12–14 are proximally presented in the same polypeptide chain. In the treatment of chronic wounds within a diabetic mouse model, this angiogenic hydrogel has also been found to greatly enhance the regenerative effects of the tested GFs.<sup>41</sup> Overall, through the use of this novel proangiogenic hydrogel, the efficacy of the growth factor is not only accentuated, but growth factor release is spatially modulated and subsequent vascularization is guided and organized.<sup>43–46</sup> As such, we sought to evaluate the potential of this system for islet transplantation, when applied within macroporous PDMS-based scaffolds.

### Implantation of PDMS scaffolds and fibrin/PDGF-BB hydrogels within syngeneic mouse model

The efficacy of syngeneic islets, loaded within PDMS macroporous scaffolds with or without fibrin/PDGF-BB hydrogels, to restore normoglycemia was evaluated at the epididymal fat pad site, see Figure 1. Three groups were compared: free islets; islets loaded within PDMS scaffolds; and islets loaded within PDMS scaffolds plus fibrin/PDGF-BB. The syngeneic model was selected to permit evaluation of engraftment efficiency in the absence of compounding factors associated with immunological rejection or the use immunosuppressive regimens. For all transplants performed, no adverse events were recorded.

All recipients of full islet mass (500 IEQ) reverted diabetes and sustained normoglycemia, irrespective of the modality

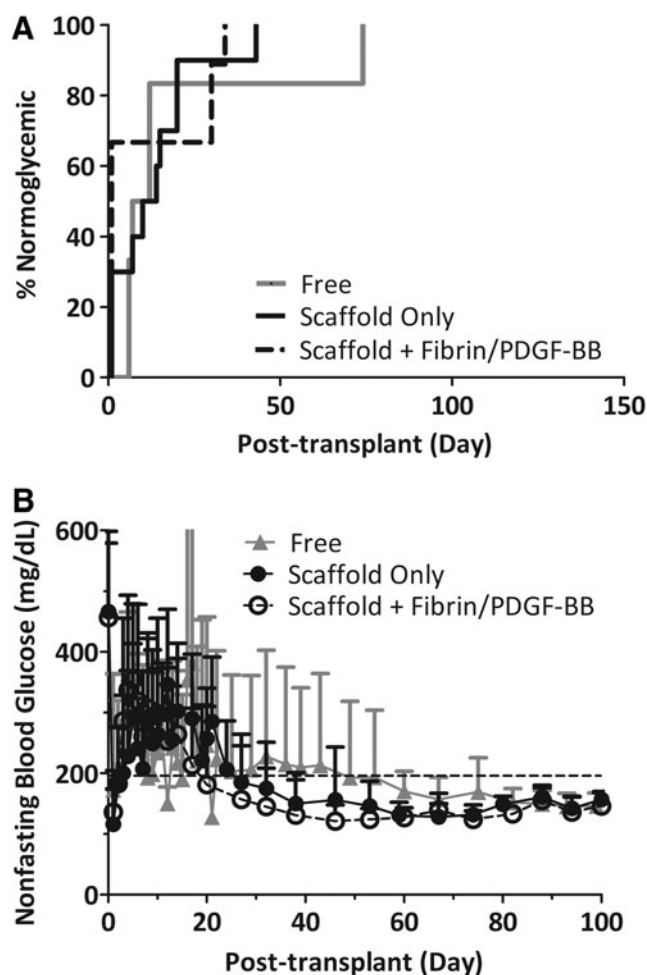


**FIG. 2.** Transplants of 500 islet equivalent (IEQ) C57BL/6J islets into diabetic C57BL/6J mouse recipients. **(A)** Time to reversal to normoglycemia and **(B)** average nonfasting blood glucose of recipients following transplantation of 500 IEQ into the epididymal fat pad either free (gray line;  $n=6$ ), within a PDMS scaffold (black line;  $n=9$ ), or within a PDMS scaffold coloaded with fibrin/PDGF-BB (dashed black line;  $n=9$ ). Reversal is defined as two consecutive readings  $<200$  mg/dL. Implants were explanted between 110 and 150 days, where prompt reversal to a diabetic state was observed for all animals. Error bars = standard deviation. No statistical difference in time to reversal was observed for any of the groups.

of the implantation (Fig. 2A). Mean reversal times for free islets (no scaffold), scaffold only, and scaffold plus fibrin/PDGF-BB were 19.5 days (7–74 days,  $n=6$ ), 11 days (1–34 days,  $n=9$ ), and 11 days (1–43 days,  $n=9$ ), respectively. At this loading, no difference in time to normoglycemia was observed between groups ( $p=0.839$ ). Following diabetes reversal, nonfasting blood glucose values for all groups were stable throughout the course of the study. Figure 2B summarizes the average nonfasting blood glucose levels. The body weight of the recipients increased following stabilization of blood glucose, indicating an improved overall metabolic state after transplantation (data not shown).

To evaluate the potential benefits of the proangiogenic hydrogel, the islet transplant load was reduced by half to 250 IEQ. As expected with this model, there was a significant delay in stabilization to normoglycemia, see Figure 3A. For islets freely loaded into the fat pad, six of the seven animals (85.7%) reverted to stable normoglycemia, with a mean reversal time of 48 days (16–56 days,  $n=6$ ). For islets within PDMS scaffolds, all eight animals (100%) reverted to stable normoglycemia, with a mean reversal time of 45 days (9–98 days,  $n=8$ ). For islets within PDMS scaffolds plus fibrin/PDGF-BB, all eight animals (100%) reverted to stable normoglycemia, with a mean reversal time of 19 days (8–25 days,  $n=8$ ). Thus, at this loading of 250 IEQ, a significant difference in the time to reversal for the PDMS scaffold plus fibrin/PDGF-BB was observed ( $p=0.045$  PDMS scaffold plus fibrin/PDGF-BB vs. free islets;  $p=0.009$  PDMS scaffold plus fibrin/PDGF-BB vs. scaffold only). Once an animal reverted, the nonfasting blood glucose values remained normoglycemic throughout the course of the study. As summarized in Figure 3B, the group containing scaffold plus fibrin/PDGF-BB exhibited statistically more stable blood glucose levels than free islets or islets within scaffolds only (i.e., the Levine's test of equality of error variance found homogeneity of variance for free islets and scaffold groups,  $p>0.104$  at all time points; while nonhomogeneity of variance was found when compared to the scaffold/fibrin/PDGF-BB group; day 20–100). Repeated measures ANOVA found significant differences between the implant type ( $p=0.017$ ) after day 20. Note that because the Mauchly's Test of Sphericity indicated rejection of assumption of sphericity ( $p<0.01$ ), a Greenhouse–Geisser correction was used. For all functional grafts, the body weight of the recipients increased following stabilization of blood glucose, indicating an improved overall metabolic state after transplantation (data not shown).

Evaluation of metabolic control via IPGTT found adequate control for all effective transplants (Fig. 3C). Clearance of bolus glucose was statistically identical for all groups, with AUC values at  $16,740 \pm 4787$ ,  $16,196 \pm 5608$ ,  $13,042 \pm 3001$ , and for free islets, islets in PDMS scaffold only, and islets in PDMS scaffolds plus fibrin/PDGF-BB, respectively.

Following removal of the fat pad, all animals reverted to the diabetic state, confirming that the transplanted grafts were responsible for the observed metabolic control.

Histological assessment of explanted islets found robust, vascularized islets, (Fig. 4). H&E staining of explanted grafts found strong infiltration of host cells and deposition of the extracellular matrix into the graft, filling the void space within the scaffold. The PDMS scaffold appeared well integrated with the surrounding tissue, with no evident fibrotic capsule or lymphocytic infiltrate. As highlighted in Figure 4,

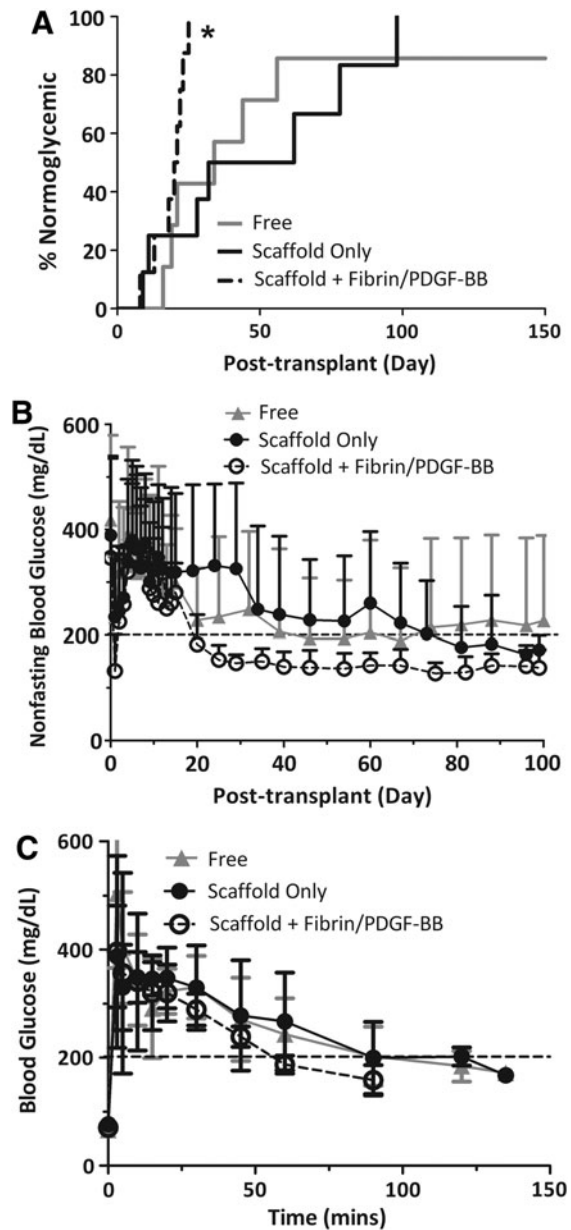


**FIG. 3.** Transplants of 250 IEQ C57BL/6J islets into diabetic C57BL/6J mouse recipients. (A) Time to reversal to normoglycemia and (B) average nonfasting blood glucose of recipients following transplantation of 250 IEQ into the epididymal fat pad either free (gray line;  $n=7$ ), within a PDMS scaffold (black line;  $n=8$ ), or within a PDMS scaffold coloaded with fibrin/PDGF-BB (dashed black line;  $n=8$ ). Reversal is defined as two consecutive readings  $<200$  mg/dL. (C) Intravenous glucose tolerance test performed on functional graft recipients at 95 days post-transplant. Blood glucose measurements were collected at time points indicated, following injection of bolus glucose, for islets in either free (gray triangle;  $n=2$ ), within a PDMS scaffold (black circle;  $n=3$ ), or within a PDMS scaffold coloaded with fibrin/PDGF-BB (dashed black open circle;  $n=3$ ). Implants were explanted between 110 and 150 days, where prompt reversal to a diabetic state was observed for all animals. Error bars=standard deviation. \*Statistically significant difference in time to reversal from both scaffold only ( $p=0.009$ ) and free ( $p=0.045$ ). No difference was observed between free and scaffold-only groups ( $p=0.90$ ).

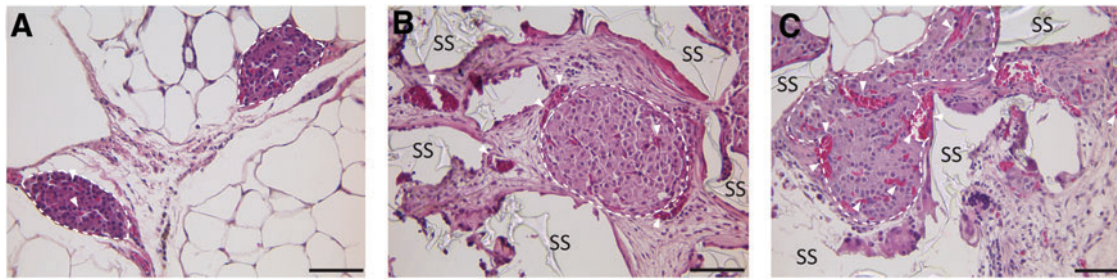


**FIG. 4.** Representative histopathological images of hematoxylin/eosin-stained islets explanted from the epididymal fat pad. (A) Free islets (day 115); (B) islets within a PDMS scaffold (day 110); and (C) islets within PDMS scaffold with fibrin/PDGF-BB (day 110); dashed lines encircle islets; white arrows highlight functional vasculature with red blood cells; SS=PDMS scaffold; scale bar=50  $\mu\text{m}$ . Color images available online at [www.liebertpub.com/tea](http://www.liebertpub.com/tea)

blood vessels were detected surrounding the embedded islets and within the islets themselves, illustrating intrascaffold and intraislet vascularization.

#### Evaluation of graft vascularization

To evaluate the effects of the fibrin/PDGF-BB proangiogenic degradable hydrogel on scaffold vascularization, competent blood vessels within the scaffold was evaluated via perfusion endothelial labeling using a lipophilic carbocyanine dye on day 10 post-transplant. A thin section was then excised from the center cross section of the fixed explanted scaffolds, thereby permitting for the evaluation of vascularization within the scaffold itself. Multislice confocal microscopy was used to visualize the stained vessels. As shown in Figure 5, competent blood vessels were observed within both scaffold groups. Of note, the vessels within scaffolds containing fibrin/PDGF-BB appeared denser and more branched, indicating greater competent vascularization of the scaffold. Sectioning of grafts without loss of the

staining was not feasible, given that PDMS scaffolds could not be frozen sectioned. While not quantifiable, these results suggest that the observed enhanced engraftment efficiency for the scaffold plus fibrin/PDGF-BB is due to enhanced overall vascularization of the graft.

Assessment of intraislet vascularization was performed on islet-loaded PDMS scaffolds, with or without fibrin/PDGF-BB explanted 10 and 30 days post-transplantation. Grafts were histologically evaluated following staining with insulin and  $\alpha$ -SMA. Obtaining clean sections of the PDMS scaffolds was exceptionally difficult, due to section folding and shearing induced by the presence of the hydrophobic PDMS material and the small size of the implant. Thus, quantification of overall graft vascularization via image analysis of stained slides was not feasible. Qualitative evaluation of individual islets, however, yields observations on intraislet vascularization. In analysis of islets within the grafts, a stronger presence of  $\alpha$ -SMA within islets containing fibrin/PDGF-BB was observed on day 10 (Fig. 6), indicating a greater presence of mature vessels within the islet. By day 30,

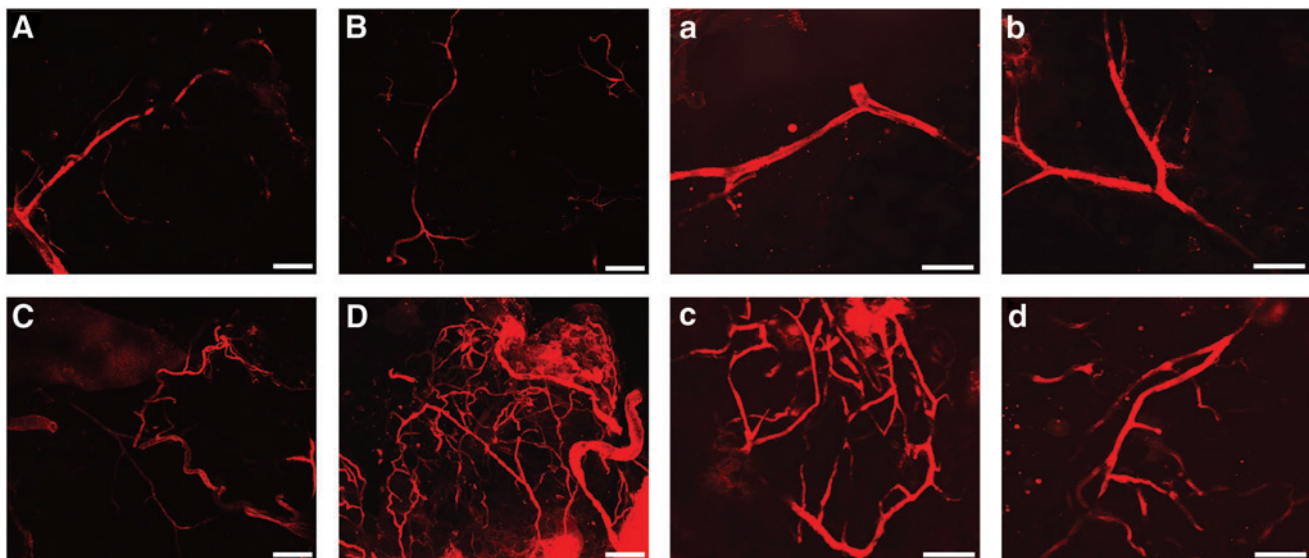


**FIG. 5.** Multislice confocal microscopy projections of lipophilic carbocyanine dye DiI within scaffold cross sections. Scaffolds contained either none (top row, A, B & a, b) or fibrin/PDGF-BB (bottom row, C, D & c, d) and were perfused with lipophilic carbocyanine dye DiI before explantation on day 10. Scale bars: 200  $\mu\text{m}$  for A–D, 100  $\mu\text{m}$  for a–d. Color images available online at [www.liebertpub.com/tea](http://www.liebertpub.com/tea)



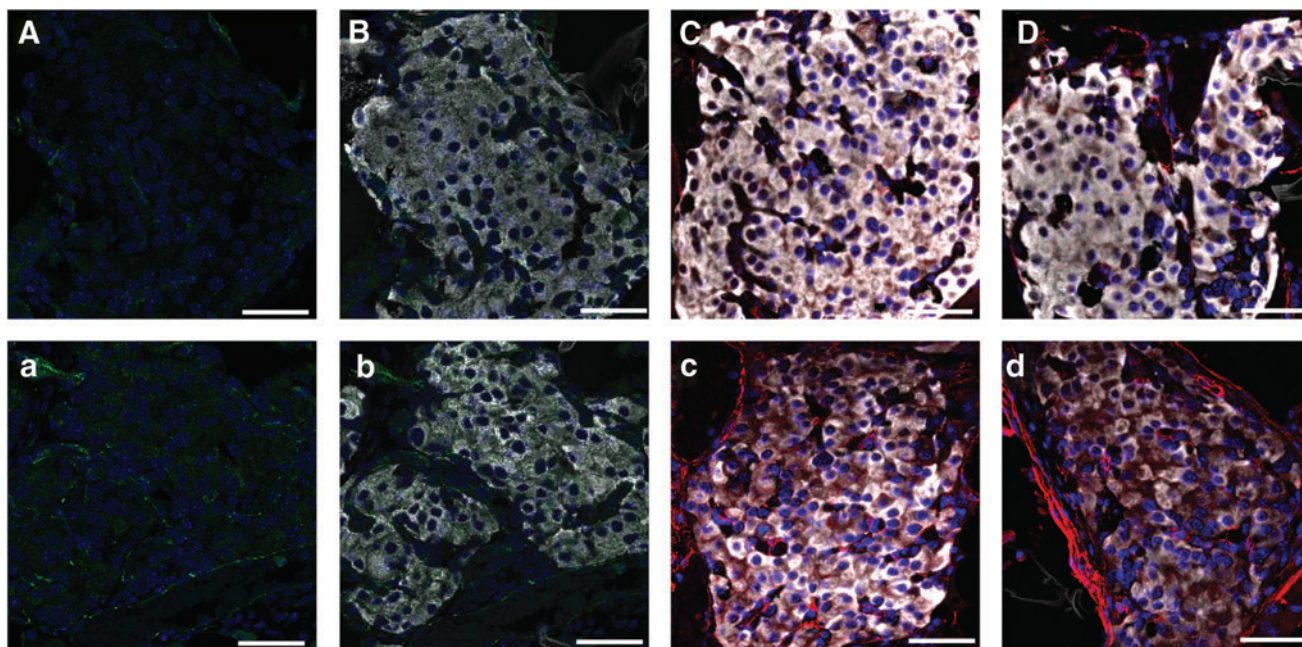


**FIG. 6.** Histopathological evaluation of islet-loaded PDMS scaffolds, removed from the epididymal fat pad site on day 10 (A–C; a–c) or day 30 (D & d), which contained either no (A–D) or fibrin/PDGF-BB (a–d). Representative images of immunofluorescence staining of explants for CD31 (green) (A & a), CD31 plus insulin (white) (B & b), and  $\alpha$ -smooth muscle actin (red) plus insulin (white) (C–D & c–d). All sections were counterstained with DAPI (blue); scale bar = 50  $\mu$ m. Color images available online at [www.liebertpub.com/tea](http://www.liebertpub.com/tea)

this trend is no longer observed, as  $\alpha$ -SMA was seen throughout islets within the scaffold-only implant. This trend further supports the hypothesis that enhanced scaffold, and subsequent islet, vascularization due to the presence of fibrin/PDGF-BB results in the observed increase in islet engraftment efficiency.

Given the importance of a competent vascular network in ensuring islet viability, function, and responsiveness, the use of proangiogenic hydrogels within scaffolds at alternative sites represents a promising approach. In this study, we found enhanced effects in islet engraftment, with a significant reduction in time to graft efficacy, when proangiogenic hydrogels were combined with macroporous scaffolds. This combinatory approach merges the benefits of a degradable biofunctional hydrogel with a biostable framework. As such, the local and spatial delivery of growth factors, as well as intradvice remodeling, is facilitated, while retention of the overall framework of the scaffold permits for retrievability and the possibility for long-term delivery of beneficial agents. While illustrating its benefits for islet transplantation, this platform has universal use in providing mechanical support and vascularization of cellular implants. Future studies are exploring the potential of this system in larger animal models, as well as the incorporation of additional agents to modulate the transplant environment.

#### Acknowledgments

This research was supported by the Juvenile Diabetes Research Center for Islet Transplantation at the University of Miami–Diabetes Research Institute (4-2004-361), the Diabetes Research Institute Foundation, the Department of Defense

Somatic Cell Processing Facility at the DRI (N00244-07-C-1529), Converge Biotech, Inc., and the European Commission project AngioScaff. E.P. was supported by an NIH NIDDK Predoctoral Fellowship (1F311EB008970-01A1). We greatly thank the Diabetes Research Institute Preclinical and Translational Models Core for providing assistance with the rodent studies, particularly Dr. R. Damaris Molano. We also thank Irayme Labrada for her technical assistance in the surgeries, as well as her expertise in immunohistochemical staining of samples. We thank Dr. Alice Tomei for sharing her CD31 staining protocol. We thank the Diabetes Research Institute Analytical Imaging Core for use of their facilities, as well as the assistance of Dr. George McNamara in image collection and processing. We thank Kevin Johnson from the Diabetes Research Institute Histology Core for his excellent skill in processing the challenging histological samples.

#### Disclosure Statement

Stockholder (AP, CR, JAH, and CLS) of Converge Biotech Inc. (Miami). EP, AP, CR, JAH, and CLS have patent applications that include the PDMS scaffolds. JAH and M.M. are inventors of patents covering the fibrin hydrogels.

#### References

1. The effect of intensive treatment of diabetes on the development and progression of long-term complications in insulin-dependent diabetes mellitus. The Diabetes Control and Complications Trial Research Group. *N Engl J Med* **329**, 977, 1993.

2. Pileggi, A., Cobianchi, L., Inverardi, L., and Ricordi, C. Overcoming the challenges now limiting islet transplantation: a sequential, integrated approach. *Ann N Y Acad Sci* **1079**, 383, 2006.
3. Shapiro, A.M., Ricordi, C., Hering, B.J., Auchincloss, H., Lindblad R, Robertson, R.P., *et al.* International trial of the Edmonton protocol for islet transplantation. *N Engl J Med* **355**, 1318, 2006.
4. Hardy, M.A., Witkowski, P., Sondermeijer, H., and Harris, P. The long road to pancreatic islet transplantation. *World J Surg* **34**, 625, 2010.
5. Cattan, P., Berney, T., Schena, S., Molano, R.D., Pileggi, A., Vizzardelli, C., *et al.* Early assessment of apoptosis in isolated islets of Langerhans. *Transplantation* **71**, 857, 2001.
6. Mattsson, G., Jansson, L., Nordin, A., Andersson, A., and Carlsson, P.O. Evidence of functional impairment of syngeneically transplanted mouse pancreatic islets retrieved from the liver. *Diabetes* **53**, 948, 2004.
7. Moberg, L., Johansson, H., Lukinius, A., Berne, C., Foss, A., Kallen, R., *et al.* Productions of tissue factor by pancreatic islet cells as a trigger of detrimental thrombotic reactions in clinical islet transplantation. *Lancet* **360**, 2039, 2002.
8. Merani, S., Toso, C., Emamaullee, J., and Shapiro, A.M. Optimal implantation site for pancreatic islet transplantation. *Br J Surg* **95**, 1449, 2008.
9. Cantarelli, E., and Piemonti, L. Alternative transplantation sites for pancreatic islet grafts. *Curr Diab Rep* **11**, 364, 2011.
10. Giraldo, J.A., Weaver, J.D., and Stabler, C.L. Tissue engineering approaches to enhancing clinical islet transplantation. *J Diabetes Sci Technol* **4**, 1238, 2010.
11. Gibly, R.F., Graham, J.G., Luo, X., Lowe, W.L., Jr., Hering, B.J., and Shea, L.D. Advancing islet transplantation: from engraftment to the immune response. *Diabetologia* **54**, 2494, 2011.
12. Borg, D., and Bonifacio, E. The Use of Biomaterials in Islet Transplantation. *Curr Diabetes Rep* **11**, 434, 2011.
13. Gibly, R.F., Zhang, X., Graham, M.L., Hering, B.J., Kaufman, D.B., Lowe, W.L., Jr., *et al.* Extrahepatic islet transplantation with microporous polymer scaffolds in syngeneic mouse and allogeneic porcine models. *Biomaterials* **32**, 9677, 2011.
14. Blomeier, H., Zhang, X., Rives, C., Brissova, M., Hughes, E., Baker, M., *et al.* Polymer scaffolds as synthetic microenvironments for extrahepatic islet transplantation. *Transplantation* **82**, 452, 2006.
15. Pedraza, E., Brady, A., Fraker, C., Molano, R., Sukert, S., Kenyon, N., *et al.* Macro-porous PDMS scaffolds for extrahepatic islet transplantation. *Cell Transplant* **22**, 1123, 2013.
16. Berman, D.M., O'Neil, J.J., Coffey, L.C., Chaffanjon, P.C., Kenyon, N.M., Ruiz, P., Jr., *et al.* Long-term survival of nonhuman primate islets implanted in an omental pouch on a biodegradable scaffold. *Am J Transplant* **9**, 91, 2009.
17. Kenyon, N., Pedraza, E., Berman, D.M., Willman, M., Kenyon, N., Margolles-Clark, E., *et al.* Scaffolds within an omental pouch site support long term survival of allogeneic, nonhuman primate islets. *Amer J Transplant* **11**, 117, 2011.
18. Pedraza, E., Coronel, M., Fraker, C., Ricordi, C., and Stabler, C. Enhancing beta-cell viability via hydrolytically activated, oxygen generating biomaterials. *Proc Natl Acad Sci U S A* **109**, 4245, 2012.
19. Song, Y., Margolles-Clark, E., Fraker, C., Weaver, J.D., Ricordi, C., Pileggi, A., *et al.* Feasibility of localized immunosuppression: 3. preliminary evaluation of organosilicone constructs designed for sustained drug release in a cell transplant environment using dexamethasone. *Pharmazie* **67**, 502, 2012.
20. Dionne, K.E., Colton, C.K., and Yarmush, M.L. Effect of oxygen on isolated pancreatic tissue. *ASAIO Trans* **35**, 739, 1989.
21. Dionne, K.E., Colton, C.K., and Yarmush, M.L. Effect of hypoxia on insulin secretion by isolated rat and canine islets of Langerhans. *Diabetes* **42**, 12, 1993.
22. Andersson, A., Korsgren, O., and Jansson, L. Intra-arterially transplanted pancreatic islets revascularized from hepatic arterial system. *Diabetes* **38 Suppl 1**, 192, 1989.
23. Ballian, N., and Brunicaardi, F.C. Islet vasculature as a regulator of endocrine pancreas function. *World J Surg* **31**, 705, 2007.
24. Miao, G., Ostrowski, R.P., Mace, J., Hough, J., Hopper, A., Peverini, R., *et al.* Dynamic production of hypoxia-inducible factor-1alpha in early transplanted islets. *Am J Transplant* **6**, 2636, 2006.
25. Moritz, W., Meier, F., Stroka, D.M., Giuliani, M., Kugelmeier, P., Nett, P.C., *et al.* Apoptosis in hypoxic human pancreatic islets correlates with HIF-1alpha expression. *Faseb J* **16**, 745, 2002.
26. Linn, T., Schmitz, J., Hauck-Schmalenberger, I., Lai, Y., and Bretzel, R.G., Brandhorst, H., *et al.* Ischaemia is linked to inflammation and induction of angiogenesis in pancreatic islets. *Clin Exp Immunol* **144**, 179, 2006.
27. Cheng, K., Ho, K., Stokes, R., Scott, C., Lau, S.M., Hawthorne, W.J., *et al.* Hypoxia-inducible factor-1alpha regulates beta cell function in mouse and human islets. *J Clin Invest* **120**, 2171, 2010.
28. Cantley, J., Grey, S.T., Maxwell, P.H., and Withers, D.J. The hypoxia response pathway and beta-cell function. *Diabetes Obes Metab* **12 Suppl 2**, 159, 2010.
29. Cabric, S., Sanchez, J., Johansson, U., Larsson, R., Nilsson, B., Korsgren, O., *et al.* Anchoring of vascular endothelial growth factor to surface-immobilized heparin on pancreatic islets: implications for stimulating islet angiogenesis. *Tissue Eng Part A* **16**, 961, 2010.
30. Park, K.S., Kim, Y.S., Kim, J.H., Choi, B., Kim, S.H., Tan, A.H., *et al.* Trophic molecules derived from human mesenchymal stem cells enhance survival, function, and angiogenesis of isolated islets after transplantation. *Transplantation* **89**, 509, 2010.
31. Johansson, U., Rasmusson, I., Niclou, S.P., Forslund, N., Gustavsson, L., Nilsson, B., *et al.* Formation of composite endothelial cell-mesenchymal stem cell islets: a novel approach to promote islet revascularization. *Diabetes* **57**, 2393, 2008.
32. Shimoda, M., Chen, S., Noguchi, H., Matsumoto, S., and Grayburn, P.A. *In vivo* non-viral gene delivery of human vascular endothelial growth factor improves revascularisation and restoration of euglycaemia after human islet transplantation into mouse liver. *Diabetologia* **53**, 1669, 2010.
33. Lai, Y., Schneider, D., Kiszun, A., Hauck-Schmalenberger, I., Breier, G., Brandhorst, D., *et al.* Vascular endothelial growth factor increases functional beta-cell mass by improvement of angiogenesis of isolated human and murine pancreatic islets. *Transplantation* **79**, 1530, 2005.
34. Langlois, A., Bietiger, W., Seyfritz, E., Maillard, E., Vivot, K., Peronet, C., *et al.* Improvement of rat islet viability during transplantation: validation of pharmacological approach to induce VEGF overexpression. *Cell Transplant* **20**, 1333, 2011.



35. Smith, J.D., Melhem, M.E., Magge, K.T., Waggoner, A.S., and Campbell, P.G. Improved growth factor directed vascularization into fibrin constructs through inclusion of additional extracellular molecules. *Microvasc Res* **73**, 84, 2007.
36. Ucuzian, A.A., Brewster, L.P., East, A.T., Pang, Y., Gassman, A.A., and Greisler, H.P. Characterization of the chemotactic and mitogenic response of SMCs to PDGF-BB and FGF-2 in fibrin hydrogels. *J Biomed Mater Res, A* **94**, 988, 2010.
37. Sakiyama-Elbert, S.E., Das, R., Gelberman, R.H., Harwood, F., Amiel, D., and Thomopoulos, S. Controlled-release kinetics and biologic activity of platelet-derived growth factor-BB for use in flexor tendon repair. *J Hand Surg Am* **33**, 1548, 2008.
38. Thomopoulos, S., Zaegel, M., Das, R., Harwood, F.L., Silva, M.J., Amiel, D., *et al.* PDGF-BB released in tendon repair using a novel delivery system promotes cell proliferation and collagen remodeling. *J Orthop Res* **25**, 1358, 2007.
39. Pileggi, A., Molano, R.D., Berney, T., Cattani, P., Vizzardelli, C., Oliver, R., *et al.* Heme oxygenase-1 induction in islet cells results in protection from apoptosis and improved *in vivo* function after transplantation. *Diabetes* **50**, 1983, 2001.
40. Martino, M.M., and Hubbell, J.A. The 12th-14th type III repeats of fibronectin function as a highly promiscuous growth factor-binding domain. *Faseb J* **24**, 4711, 2010.
41. Martino, M.M., Tortelli, F., Mochizuki, M., Traub, S., Ben-David, D., Kuhn, G.A., *et al.* Engineering the growth factor microenvironment with fibronectin domains to promote wound and bone tissue healing. *Sci Transl Med* **3**, 100ra89, 2011.
42. Li, Y., Song, Y., Zhao, L., Gaidosh, G., Laties, A.M., and Wen, R. Direct labeling and visualization of blood vessels with lipophilic carbocyanine dye DiI. *Nat Protocols* **3**, 1703, 2008.
43. Hubbell, J.A. Materials as morphogenetic guides in tissue engineering. *Curr Opin Biotechnol* **14**, 551, 2003.
44. Hubbell, J.A. Materials science. Enhancing drug function. *Science* **300**, 595, 2003.
45. Lutolf, M.P., and Hubbell, J.A. Synthetic biomaterials as instructive extracellular microenvironments for morphogenesis in tissue engineering. *Nat Biotechnol* **23**, 47, 2005.
46. Zisch, A.H., Zeisberger, S.M., Ehrbar, M., Djonov, V., Weber, C.C., Ziemiecki, A., *et al.* Engineered fibrin matrices for functional display of cell membrane-bound growth factor-like activities: study of angiogenic signaling by ephrin-B2. *Biomaterials* **25**, 3245, 2004.

Address correspondence to:

Cherie L. Stabler, PhD

Department of Biomedical Engineering

University of Miami

1450 NW 10th Avenue

Miami, FL 33136

E-mail: cstabler@med.miami.edu

Received: November 19, 2012

Accepted: June 19, 2013

Online Publication Date: August 7, 2013